INVESTIGATIONS OF DEFECT CENTRES IN ALKALI HALIDES DOPED WITH TRIVALENT CATIONS. PART 2: THE NaCl:Cr^{3+} CRYSTALS

M. Suszyńska

W. Trzebiatowski Institute of Low Temperature and Structure Research
Polish Academy of Sciences
Pl. Katedralny 1, 50-950 Wrocław, Poland

AND R. Capelletti

Physics Department, Parma University, 43100 Parma, Italy

Dedicated to Professor Dr. Julian Auleytner
on the occasion of his 70th birthday

On the basis of ITC studies, complemented by some spectroscopic and ionic conductivity measurements, it was stated that dielectric relaxations of the NaCl:Cr^{3+} crystals are more complicated than those typical of AH:Me^{2+} systems. The complexity of these phenomena concerns the number, shape and positions of the bands appearing in the ITC spectrum. The origin of the main peaks was discussed in terms of relaxations related with the chromium centres; substitutionally and off-center located Cr^{3+} ions, accompanied by two cation vacancies at geometrically different positions, and Cr clusters distributed around dislocations were considered.

PACS numbers: 77.40.+i

1. Introduction

The present series of papers, devoted to alkali halides (AH) doped with "small" trivalent cations (Me^{3+}), began with characterization of bismuth centres in NaCl, KCl and RbCl crystals (Part 1 [1]). Although some evidences for the presence of impurity–vacancy–vacancy (I.V.V.) dipoles were gathered, bismuth affinity to oxygen-like anions made the quantitative analysis of the obtained results difficult.

Similar to bismuth doped crystals the impurity related defects in chromium doped NaCl crystals were mainly studied by ionic thermocurrent (ITC) technique

employed in an extended range of temperature for samples doped in a wide range of concentration, c_{3+}. In parallel, EPR spectra and the temperature dependence of ionic conductivity were also investigated. It should be noted that trivalent chromium is especially interesting for these studies because of laser and solar collector applications [2]. Moreover, for $NaCl:Cr^{3+}$ crystals the ratio of ionic radii r_{3+}/r_+ is still smaller than for the bismuth doped AH, and still more similar to doped silver halides with the structure of sodium chloride. For this reason, the results obtained are critically compared with those presented by Ulrici [3] and Kunze et al. [4] for silver halides doped with trivalent chromium; the most characteristic features of ITC spectra typical of $AH:Me^{2+}$ systems with $r_{2+} \geq r_+$ were also shortly discussed.

2. Crystals and techniques used

2.1. Basic characteristics of samples

Single crystals of NaCl containing trivalent chromium ions were grown by a modified Bridgman method [5] at the Crystal Growth Laboratory, Institute of Physics, CSAV, Prague by Dr M. Lebl.

The nominal concentration of the dopant ranged between 10 and 2000 mole ppm. The chromium content was determined by the atomic absorption spectrometry (AAS), whereby a Perkin–Elmer spectrometer was used; for the numerical data see Table I.

TABLE I

Characterization of crystals.

Mark	Dopant [ppm]		Remarks
	Melt	AAS/OA	
F.1	10	4.5/–	1. $r(Cr:3+) = 0.63$ Å,
F.2	30	–/0.38	$r(Na:+) = 0.98$ Å,
F.5	300	–/0.38	$r = 0.63/0.98 = 0.64$.
F.6	500	14/1.04	2. Cr(3+) and Cr(+)
F.7	800	–/1.60	ions are paramagnetic.
F.8	1000	–/1.72	3. OA gives the absorption
F.9	2000	40/2.80	coefficient at $\lambda \cong 234$ nm.

The major part of experiments was performed for as received (AR) about 15 years old crystals. In some instances the effect of high-temperature treatment was studied. After 30 minutes of annealing at 873 K the sample was dropped onto a copper plate at room temperature (RT); this procedure was considered as determining the solution treated (ST) state of samples.

2.2. ITC and other measurement techniques

If not otherwise stated, the ionic thermocurrent (ITC) measurements were performed under conditions usually applied for detection of the impurity–vacancy (I.V.) dipoles in alkali halides doped with divalent cations [6]. Additionally to the low-temperature phenomena, polarizations appearing above RT were registered. The effect of plastic deformation (uniaxial compression in a self-made device) upon the ITC spectra was detected for an arrangement described previously [7].

The valency of the dopant was systematically verified by taking the EPR spectra at RT and/or liquid nitrogen temperature (LNT) with the VARIAN-V-4502-12 spectrometer operating with 100 kHz field modulation. The orientation of samples was achieved by means of a goniometer, and for the purposes of this work the samples were rotated around angle Θ between the magnetic field and the main crystal axes.

The temperature dependence of ionic conductivity was measured in the same way as it has been described in Part 1 [1].

3. Results and discussion

3.1. Ionic conductivity

Figure 1 shows the conductivity σ versus inversion of temperature $1/T$ for AR samples doped with various amounts of chromium.

Similar to bismuth doped NaCl crystals (Part 1) the temperature dependence of σ displays two characteristic regions, the extrinsic and association one. Hence, the conductivity plots of slightly doped samples are explainable in terms of substitutionally incorporated Cr^{3+} ions for which the charge excess is compensated by cation vacancies. With increasing c_{3+} the association of vacancies occurs at temperatures at which the intrinsic conductivity takes place. Similar to the bismuth doped alkali halides [1], the number of cation vacancies, induced by each Cr^{3+} ion, is larger than one. The migration and association energies, obtained from the $\lg(\sigma T)$ vs. $1/T$ plot for AR samples, are listed in Table II; for comparison, experimental data for NaCl crystals doped with other transition metal ions are also presented. The values obtained are similar to each other, whence the effect of electric charge seems rather poor, at least for the migration. This result is in contrast with the classical theory by Tosi and Doyama [10] in which the charge as well as size of the dopant are strongly involved.

3.2. EPR spectra

For heavily doped samples the EPR spectra detected at RT are composed of different lines, whose number increases with decreasing temperature. The large number of lines is probably the consequence of several overlapping spectra related with several paramagnetic centres, whose g-factor takes an average value of 2.0036.

To obtain information about the symmetry and/or the relative number of centres, preliminary studies of the signal anisotropy were undertaken. The crystals
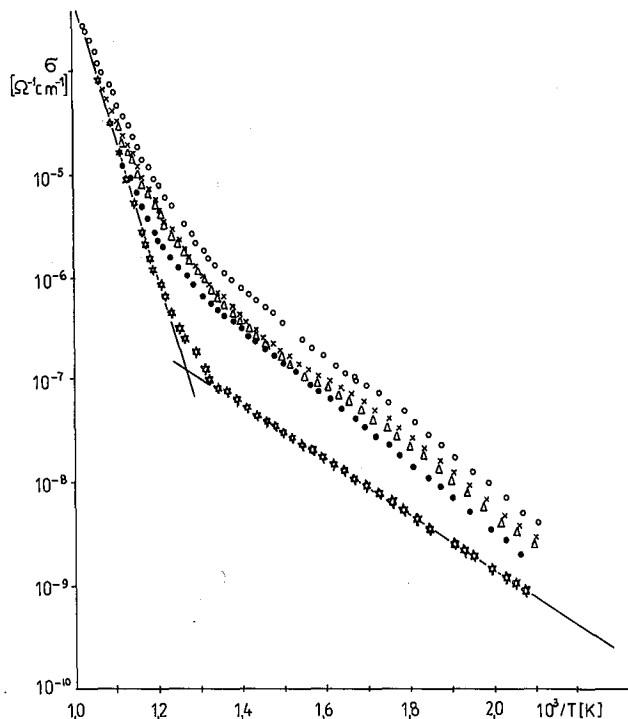
Fig. 1. Temperature dependence of the electric conductivity of AR samples doped with 30 (•), 300 (△), 800 (×) and 2000 (o) mole ppm of Cr(3+); curve (*) shows data characteristic of nominally pure NaCl crystals.

were rotated in (100) and (110) planes by 2.5 angular degree. Figure 2 exemplifies the results obtained by rotating the F.3 crystal about a ⟨100⟩ direction. Although

TABLE II

Activation energies of Cr(3+) ions compared with those characteristic of some transition metal ions incorporated substitutionally in NaCl crystals.

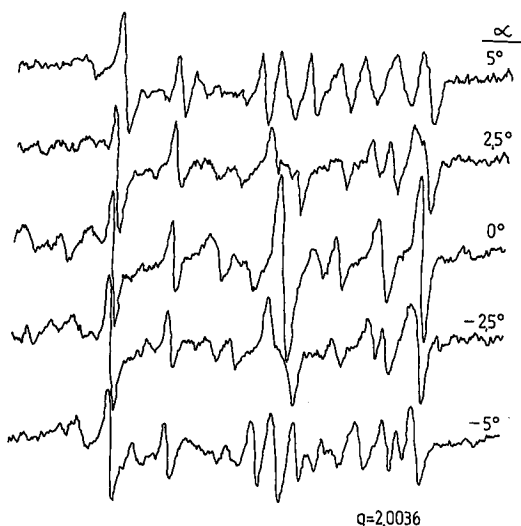| Ion	Energy of		Refs.
	association	migration	
Mn(2+)	0.3 ÷ 0.6	0.8 ÷ 0.95	[8]
Ni(2+)	0.32, 0.62	0.75	[9]
Co(2+)	0.3	0.75	[9]
V(2+)	0.43	0.7	[9]
Cr(3+)	0.68	0.78	here

Fig. 2.   Room-temperature EPR spectra of the F.3 sample showed for various values of α — the angle between the [100] direction and the magnetic field H; sweep frequency $\cong 100$ Hz.
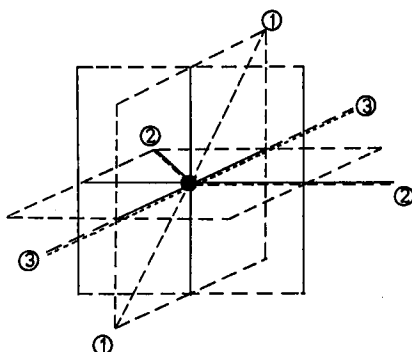

Fig. 3. Cr^{3+} in the NaCl matrix, associated with two vacancies in the nn and nnn positions. The symmetries D_{2h}, C_s and D_{4h} are represented by vacancy pairs labelled 1, 2 and 3 respectively; black point marks the Cr(3+) ion position.

the observed spectra were not analysed in sufficient details to fit an appropriate Hamiltonian, the angular dependence of the position of some spectral lines can be related with centres of a twofold and a fourfold symmetry. These symmetries are characteristic of defects composed of the impurity ions and cation vacancies in the nearest neighbour (nn) and next nearest neighbour (nnn) position, respectively. Figure 3 shows the most probable configurations of I.V.V. dipoles. The symmetry of these centres could be as follows:

1. D_{2h} with two vacancies in the nn position to Cr^{3+} and in transposition to each other;

2. C_s — which arises when one vacancy is in the nn site and the other one in the nnn position, whereby both dipole axes are in the same [100] plane; and

3. D_{4h} — when both vacancies occupy the nnn sites in the transposition to each other.

Since two cation vacancies repel each other by the Coulombic interactions, the D_{2h} and other configurations with both vacancies in the nearest neighbour sites to each other are less probable. The relative number of various dipoles depends on the dopant concentration, thermal pretreatment and plastic deformation of samples; more detailed data will be reported shortly.

3.3. ITC data

3.3.1. The results obtained

The depolarization currents of NaCl:Cr(3+) crystals show a peak near 226 K ($A.1$) accompanied by another one at 206 K ($A.2$) and a broad high-temperature band (C). For the low-temperature range the effects of polarization conditions are shown in Fig. 4 for AR (curves 1 and 2) and ST samples of the F.6 crystal (the remaining curves). Figure 5 shows the most characteristic features of the low- and high-temperature bands. On assuming that the temperature dependence of the relaxation time related with the low-temperature band is of Arrhenius type, the activation parameters for reorientation jumps may be calculated. Because of some experimental limitations, the activation energy E was evaluated according to Chen's approximations [11], whereas the frequency factor τ_0 was calculated from the following equation describing the condition for the band maximum:

$$T_m = [(E/k)b\tau(T_m)]^{1/2}.$$

For the Arrhenius-type jumps:

$$\tau = \tau_0 \exp(-E/kT_m),$$

and

$$\tau_0 = T_m^2 k/Eb \exp(E/kT_m)$$

with b and k denoting the heating rate (in our experiments equal to 0.1 K s^{-1}) and Boltzmann constant, respectively. Table III lists the numerical values of E and τ_0, and Fig. 6 shows the reorientation energy of Cr dipoles compared with those characteristic of divalent impurities in NaCl crystals as function of their ionic radius.

The main features of the C band may be summarized as follows:

1. The amplitude H^C and peak position T_m^C are increasing functions of the thickness of samples X.

2. For fixed X the T_m^C value depends on the polarization conditions, i.e. the polarizations related with this band should be described by a distribution of relaxation times, being meaningful for shape- and/or size distribution of particles segregated near dislocations, cp. Part 1 [1].
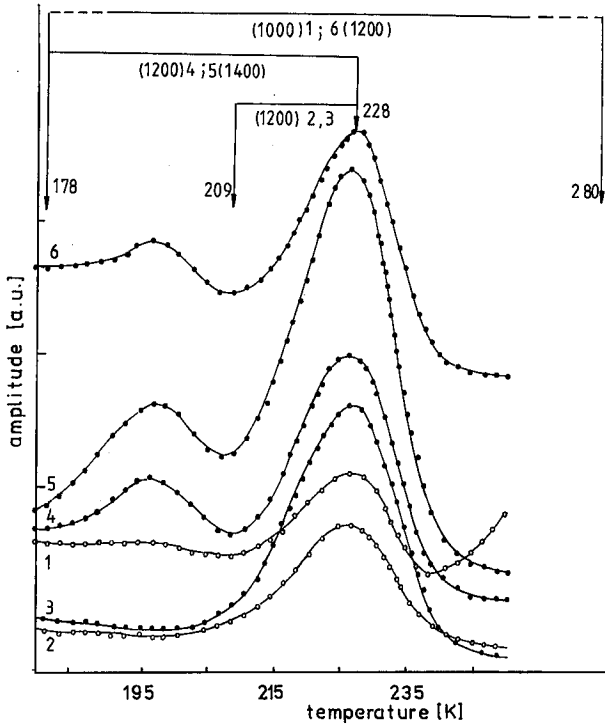
Fig. 4.   ITC spectra characteristic of the F.6 sample; the effect of polarization conditions for AR (curves 1, 2) and ST samples (remaining curves) is shown.
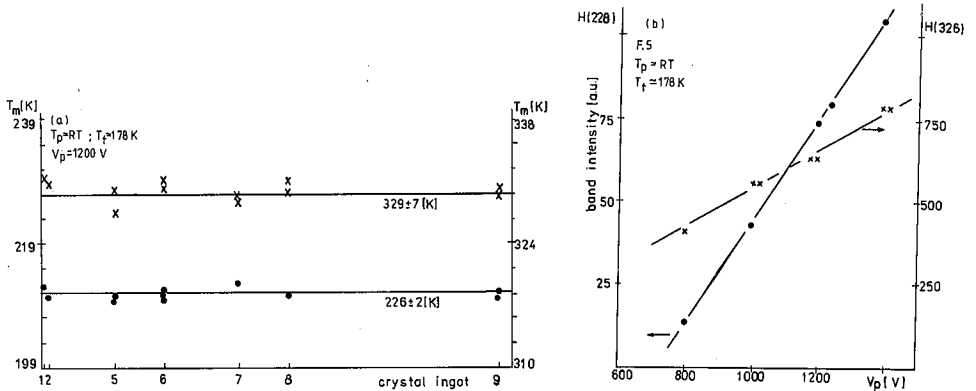

Fig. 5.   Characteristic peak positions for the crystals studied (a) and the dependence of peak amplitudes on the electric field applied (b).
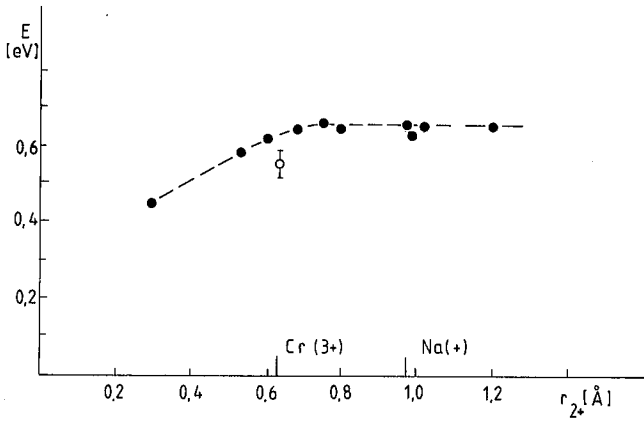
M. Suszyńska, R. Capelletti

Fig. 6. Reorientation activation energy of I.V. dipoles in NaCl crystals vs. ionic radius of divalent impurities according to [12]; the average values obtained for NaCl:Cr(3+) are also presented.
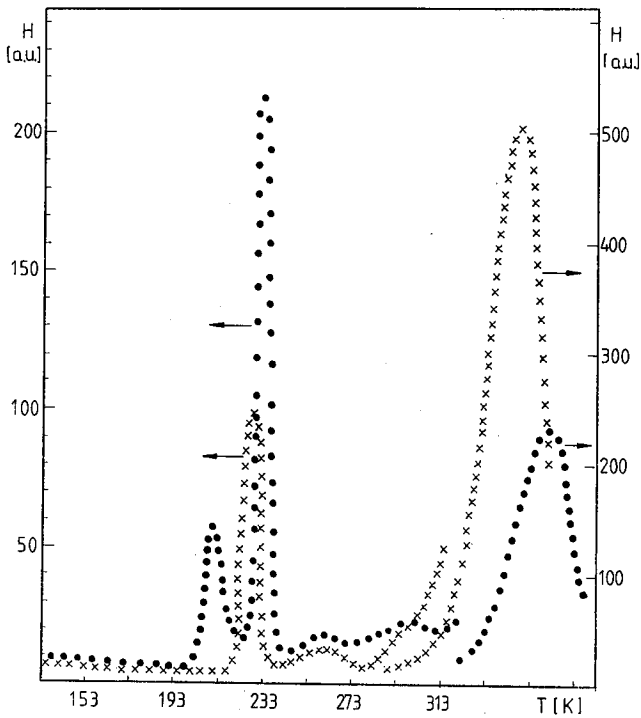

Fig. 7. Effect of plastic deformation upon ITC spectrum of the F.2 sample (●); for comparison the spectrum of AR sample is also presented (×). $T_p \cong RT$, $T_f = 178$ K, $V_p = 1460$ V.

3. Similar to the dipolar bands, the frozen-in polarizations (represented by H^C) are linear with $E_p(= V_p/X)$ up to about 3×10^3 V cm^{-1}.

4. Few percent of plastic deformation (ε) induces strong decrease in H^C, distinct shift of T_m^C towards higher values and drastic increase in the bandwidth, see Fig. 7, where data for $\varepsilon = 0$ % are shown for the sake of comparison.

TABLE III

Relaxation parameters characterizing the low-temperature ITC bands for plate-shaped and parallelepipeds in as received, aged after solution treatment and deformed samples of NaCl containing various amounts of Cr(3+) ions.

Mark	F.6.6	F.7.1	F.8.1	F.9.8	F.9.8
Shape	parall.	plate	plate	parall.	parall.
Treatment	AR + 13.3%	ST + aged/RT	ST + aged/ST	ST + 4.56%	ST + 4.56%
T_m [K]	211.5	211	213	206	182
$\mu = \frac{T_2 - T_m}{T_2 - T_1}$	0.40	0.44	0.42	0.44	0.50
E_α [eV]	0.56	0.52	0.56	0.56	0.49
E_δ [eV]	0.50	0.47	0.55	0.51	0.35
E_ω [eV]	0.54	0.50	0.56	0.54	0.42
$\langle E \rangle$ [eV]	0.53	0.50	0.56	0.54	0.42
$\tau_{0\alpha}$ [s]	4.16×10^{-12}	2.53×10^{-11}	3.16×10^{-12}	1.54×10^{-12}	1.69×10^{-12}
$\tau_{0\delta}$ [s]	8.52×10^{-11}	5.50×10^{-10}	8.70×10^{-12}	2.53×10^{-11}	1.91×10^{-8}
$\tau_{0\omega}$ [s]	1.23×10^{-11}	8.37×10^{-11}	3.70×10^{-12}	4.15×10^{-12}	1.83×10^{-10}
$\langle \tau \rangle$ [s]	1.72×10^{-11}	1.05×10^{-10}	4.69×10^{-12}	5.55×10^{-12}	1.83×10^{-10}

3.3.2. Considerations of the relaxation phenomena

The low-temperature band $A.1$ is located in the temperature range where the dipolar band occurs for AH crystals doped with small Me^{2+} ions. Although the amplitude of this band is linearly dependent on the polarization voltage, its shape is slightly different from the nonsymmetrical one characteristic of I.V. dipoles. The broadening observed with increasing c_{3+} probably reflects various geometrical configurations of coexisting I.V.V. dipoles. If so, the α-approach, practically insensitive to the kinetics order, should be considered as the best estimation of the activation energy value. The increase in c_{3+} induces not only the broadening of the main low-temperature band but also the appearance of a second band ($A.2$) positioned below the main one. This phenomenon resembles the situation in silver halides doped with trivalent chromium for which the presence of nn and nnn types of dipoles was suggested [4]. It should be noted, however, that for NaCl:Cr^{3+} crystals the $A.2$ band appears also in solution treated and plastically deformed samples. These "agents" induce lattice distortion around the Cr^{3+} ion, which might be interpreted as equivalent to an off-centre position. Since the dipolar moment of such defects is smaller than for the centrally located cations, see [13], the amplitude of both low-temperature bands is not simply proportional to the dopant concentration.

Although the behaviour of the high-temperature part of the spectrum is explainable in terms of the Maxwell–Wagner polarizations, some features of these

bands are distinctly different from those detected for AH:Me^{2+} systems [7]. It seems reasonably to assume that in the case of small trivalent cations, both the extended and compressed regions near edge dislocations are accessible for the impurities, and instead of the formation of a classical Cottrell atmosphere (typical of AH:Me^{2+} systems) an "unlimited" number of cations may be segregated here, probably in the form of aggregates and/or precipitates.

4. Concluding remarks

The main conclusion of the EPR studies — that in NaCl:Cr^{3+} crystals may coexist centres of different configuration — was confirmed by the composed character of ITC bands. Also the suggestion from conductivity data — that more than one cation vacancy accompanies the substitutionally positioned Cr^{3+} ion — found further support in the geometry of dipolar centres related with the low-temperature dielectric relaxations.

Comparing the features of the polarization phenomena detected with those typical of AH:Me^{2+} crystals with $r_{2+} \geq r_+$, some differences were found. They concern the number, shape and position of the relaxation bands appearing in the low-temperature range. Also the high-temperature bands react differently to plastic deformation and thermal pretreatment as well. In a given sense the spectra appearing in NaCl:Cr^{3+} also differ from those recently described for LiF:Ti^{3+} crystals (with $r_{3+} \geq r_+$) [14]. On the contrary, some similarities with the behaviour of the off-centre positioned Be^{2+} ions in NaCl and KCl crystals [13] and the substitutionally located Cr^{3+} ions in silver halides [4] were detected. Hence, it seems reasonable to suppose that the size of the impurity ion plays an important role in determining the main features of the polarizations registered by the sensitive ITC technique. Taking into account the conductivity data, this means that the second charge compensating cation vacancy is probably at a distance different from the considered nn and nnn ones. The evidences could be attained by studies of the EPR anisotropy. Moreover, the distribution of cation vacancies around Cr^{3+} ions and the electrostatic interactions between them should influence the degeneracy and activity of electronic and vibrational transitions as well. Hence, also spectroscopic investigations could be the basis for final determination of the structure of defects investigated.

Acknowledgments

References

[1] M. Suszyńska, R. Capelletti, *Acta Phys. Pol. A* **83**, 25 (1993).

[2] L.M. Andrews, *J. Lumin.* **24/25**, 877 (1981).

[3] W. Ulrici, *Phys. Status Solidi* **27**, 489 (1968).

[4] K. Kunze, P. Müller, *Phys. Status Solidi* **38**, 271 (1970).

[5] R. Voszka, J. Tarjan, L. Berkes, J. Krajsovszky, *Krist. Technik* **1**, 423 (1966).

[6] C. Bucci, R. Fieschi, G. Guidi, *Phys. Rev.* **148**, 816 (1966).

[7] M. Suszyńska, R. Capelletti, *Cryst. Res. Technol.* **19**, 1489 (1984).

[8] F. Beniere, R. Rokbani, *J. Phys. Chem. Solids* **36**, 1151 (1975).

[9] M. Hartmanova, M. Lebl, E. Mariani, *Phys. Status Solidi A* **31**, k 85 (1975).

[10] M.P. Tosi, M. Doyama, *Phys. Rev.* **151**, 642 (1966).

[11] R. Chen, *J. Mater. Sci.* **11**, 1521 (1976).

[12] R. Capelletti, in: *Defects in Solids*, Eds. A.V. Chadwick, M. Terenzi, Plenum, London 1986, p. 407.

[13] C. Bucci, *Phys. Rev.* **164**, 1200 (1967).

[14] R. Capelletti, M.G. Bridelli, M. Friggeri, G. Ruani, in: *Proc. 5th Symp. Electrets, IEEE, Heidelberg (Germany) 1985*, IEEE, New York 1985, p. 294.